Enhanced reflectivity contrast in confocal solid immersion lens microscopy

Khaled Karrai[a] and Xaver Lorenz
Center for NanoScience, Sektion Physik der LMU, Geschwister-Scholl-Platz 1, 80539 Munich, Germany

Lukas Novotny
The Institute of Optics, University of Rochester, Rochester, New York 14627

(Received 11 July 2000; accepted for publication 19 September 2000)

The reflected image of a diffraction limited focused spot is investigated using confocal solid immersion microscopy. We find that the spot's image shows aberrations when reflected off objects with optical indexes lower than that of the solid immersion lens (SIL) material. We demonstrate that such aberrations are only apparent and that the actual size of the spot at the SIL/object interface remains diffraction limited. The aberrations are due to lateral waves at the SIL surface. These von Schmidt waves originate from the total internal reflected components of a diverging spherical wave front. We make use of this image aberration in conjunction with the spatial filtering inherent to confocal microscopy in order to dramatically enhance the optical contrast of objects with low optical indexes. © *2000 American Institute of Physics.* [S0003-6951(00)00447-2]

Solid immersion microscopy (SIM) is a diffraction limited imaging technique that provides an enhanced spatial resolution taking advantage of the large optical index n of a solid immersion lens (SIL) objective.[1] The enhancement in the resolution is obtained by forming a diffraction limited focused light spot directly at the flat SIL/object interface. This way the size of spot scales like λ/n, where n can be as large as 3.4 when using SILs made out of gallium phosphide.[2] Such a reduction in the focused spot size has led to advances in optical disk storage schemes[3] with fast read out rates for addressing media with very high bit density.[4] The prospect of using such lenses in combination with a shorter wavelength blue semiconductor laser diode makes SIM potentially very attractive not only for data storage devices but also in the area of large light throughput superresolution optical microscopy[5] and spectroscopy.[6] Moreover, SIM can be made even more powerful when combined with confocal scanning optical microscopy techniques.[7] However, a particularity of SIM in comparison to a more common liquid immersion setup, is that the optical index of the investigated object can be smaller than that of the SIL material. This is specially the case for biological materials directly prepared on the SIL flat face. In this situation, the plane wave components of the focused wave undergo total internal reflection when impinging the SIL/object interface above a critical angle. Total internal reflection (TIR) produces local evanescent waves in the vicinity of the focal point, an aspect which is often put forward in the literature[1,3,5,7,8] extending SIM to near field optical microscopy techniques. However TIR is also accompanied by an inseparable combination of more subtle phenomena such as the Goos–Hänchen reflected beam displacement[9] and the von Schmidt's lateral waves,[9,10] both of which stem from the slower wave propagation velocity in the SIL material. In the Goos–Hänchen effect, the photons which are tunneling into the lesser optically dense object medium re-emerge into the SIL laterally displaced from the impinging point. This produces a lateral beam shift of the total internal reflected plane wave components.[9,11] The von Schmidt's lateral waves, well known in seismology, trail the diverging reflected wave components originating from the focused spot in the form of a conical wave front in a way similar to the Mach cone in fluid dynamics.[9,10] While a spherical wave front is optimally imaged into a point, a conical wave front instead is imaged into a torroid.[12] Such effects which generate aberrations in the reflected image of the focused spot have not yet been considered in the published literature on SIM. We have found that indeed such TIR related effects lead to a sizeable aberration in the image formation of the focused spot. We demonstrate in this work that luckily this apparent aberration does not affect the actual size of the probing focused spot. Furthermore, it can be used in conjunction with confocal microscopy in order to greatly enhance the reflected image contrast of low optical index objects.

Our experimental arrangement is shown in Fig. 1. A HeNe laser beam is launched in a monomode optical fiber

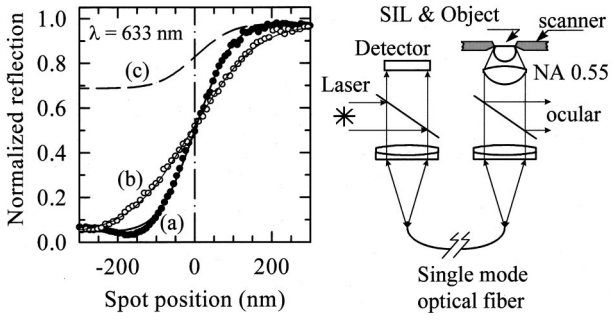

FIG. 1. (Right) Schematic of the reflection confocal scanning solid immersion microscope. (Left) Normalized reflection profile from the edge of an Al film directly evaporated on the exit flat face of the SIL. High reflectivity corresponds to the focused spot positioned over the Al film (a) was measured with the SIL (FWHM = 178 nm); (b) with a normal 0.95 NA microscope objective (FWHM = 305 nm), and (c) is the expected total reflectivity calculated including the total internal reflection components but ignoring the corresponding aberrations.

[a]Author to whom correspondence should be addressed; electronic mail: khaled.karrai@physik.uni-muenchen.de

[numerical aperture (NA) 0.12)] of which the other end serves as a diffraction limited Gaussian point source with an unspecified polarization. The beam is collimated and then focused on the SIL with an 0.55 NA Nikon microscope objective with a 4.4 mm working distance. The collimated beam waist radius (defined at $1/e$ of the intensity) corresponds to 2/3 of the stop aperture radius of the Nikon objective. A $R=5$ mm radius superhemispherical glass (LASFN9) SIL has its flat end at a plane located at R/n from the sphere center as described in Ref. 3. The lens was designed with $n=1.845$ for the operation at wavelength $\lambda=632.8$ nm. The SIL is mounted on a high precision linearized piezoelectric scanner, which allows us to position the lens with respect to the optical axis of the rest of the optics. As reported previously,[3] a Δx lateral displacement of the lens leads to a $\Delta x/n^2$ of the focal spot at the SIL object interface. This way, a lateral x or y effective scan of the spot over 14.7 μm is achievable for image formation. Similarly a longitudinal displacement Δz of the SIL along the optical axis shifts the spot only by $\Delta z/n^3$. The reflected light makes its way back to the optical fiber, which in this direction operates as a pinhole. The optical arrangement is hence confocal. A beam splitter is mounted before the fiber for visual inspection of the spot. The SIL used for the data shown in Fig. 1 was prepared with a 50 nm thin Al film covering half of its flat face. The rest of the SIL is exposed to air. The spot was scanned across the metal edge. The expected step shaped signal is fitted with an error function corresponding to a Gaussian shaped spot with a full width at half maximum (FWHM) of 178 ± 3 nm. The size of the diffraction limited spot at the SIL/object interface is expected to be 216 nm, as determined numerically for a truncated illuminating Gaussian beam. A reduction of the measured spot size by a factor $\sim(3/2)^{1/2}$ would be in agreement with the confocal arrangement using both a Gaussian illumination and pinhole functions.

In spite of this satisfactory agreement, we found that the measured contrast in reflectivity between the SIL/air and SIL/Al region (i.e., ~0.08:1) is much larger than expected from a simple derivation (i.e., ~0.7:1). A large proportion of the beam impinging on the SIL/vacuum interface which should be totally internally reflected does not reach the photodetector. We used the full Fresnel reflection coefficients weighted with the truncated Gaussian profile of the beam to simulate the expected reflected signal. The result is shown in plot(c) of Fig. 1. The disagreement with the measured data is so large that we were prompted to have a direct visual inspection of the reflected spot. We observed that when the spot was reflected off the metal film, the image was that of a diffraction limited spot. When the focused spot was laterally shifted across the metal edge over the SIL/air interface, its image appeared suddenly much larger and blurred with a minimum of intensity in its center region. Because of the spatial filtering of the collected reflected light in the confocal arrangement, the measured reflectivity appears much weaker than expected. The measurement was reproduced using a SIL with Al nanoparticles directly deposited over its flat face. The scanned image is shown in Fig. 2. The spot FWHM was found to be 190 nm. However here again we find a totally unexpected enhanced reflectivity contrast. The same observation was made for several other metal particles. Furthermore, all images showed a shadowing around the bright particle reflection sometimes with complex patterns. This enhanced reflectivity contrast could make the task of estimating the actual spot size potentially difficult should its dependence with n be nonlinear. For this reason we have also imaged a purely dielectric object with weak contrast in n and for which TIR contributions are present independently of the spot position.

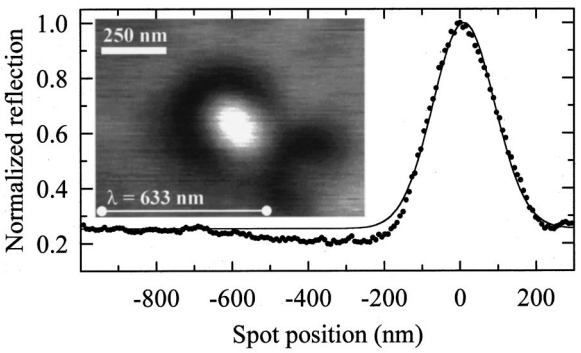

FIG. 2. Confocal scanning solid immersion microscope image of an Al particle directly deposited on the flat face of the SIL. A Gaussian linefit shows a FWHM of 190 nm.

The object is a monolayer array of densely packed 305 nm diam spherical latex beads. The beads, which contain 69% water and the rest polymer chains, have an optical index close to that of water. The space between them is likely to be filled with a water layer condensed from the environmental humidity in the laboratory. The sample is therefore not only expected to show a rather weak contrast in reflectivity but is less reflecting at the position of the beads due to a better index matching as well as reduced total internal reflection. The measurements in Fig. 3 shows the exact opposite. The contrast in the normalized reflectivity was found to be 0.2–1 in average between adjacent beads and the signal was always maximum at the beads position, indicating that here as well, the contribution of the TIR components of the focused spot are filtered away. The resolution of the image is consistent with a diffraction limited probing spot.

At this point we are confident that the enhanced contrast observed in confocal solid immersion microscopy is due to the spatial filtering of the aberrated reflected spot. The spot

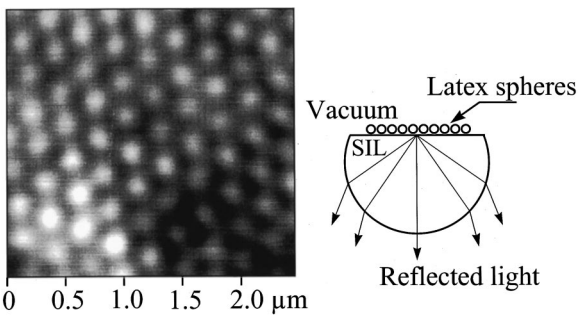

FIG. 3. Confocal scanning solid immersion microscope image (left) of an array of latex spheres (305 nm) directly deposited on the flat face of the super hemispherical SIL as schematised (right). Bright spots corresponds to high reflectivity and to the position of the spheres. The reflection intensity contrast between two neighboring spheres is about a factor of 4 in average. Naively one expects an inverted contrast when considering a reduction of totally internal reflected energy from the latex spheres.

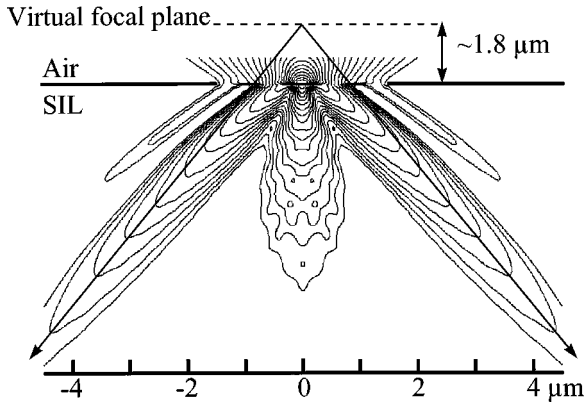

FIG. 4. Full vector field model calculation showing a contour map of the magnitude of the Poynting vector of the reflected light near focus. The intensity changes by a factor 2 between successive lines. The reflected light above critical angle appears to originate from a virtual focal plane located out side the SIL, leading to a torroidal shape of the reflected spot. Note that the focused spot is diffraction limited at the SIL/vacuum interface.

image aberration is not inherent to solid immersion microscopy. In fact Lehmann and Maecker measured it about half a century ago in a very ingenious but little known optical experiment[12] using a 1.3 NA oil immersion. In this way they proved Maeker's prediction of a torroidal aberration of the image of a totally internal reflected diffraction limited point source.[13] The effect was interpreted in terms of von Schmidt's lateral waves inherent to the total internal reflection of diverging spherical waves. In essence the resulting aberration should be understood in terms Goos–Hänchen reentrant displaced waves for the case of a spherical wave front. The question whether or not such aberrations affect the real shape of the local illuminating spot was however prior to this work still unanswered.

We have performed a rigorous vector electromagnetic field model calculation in the vicinity of the focal spot. Shown in Fig. 4 is a map of the intensity of the Poynting vector for the transmitted and reflected field. We calculated that the real focal spot does not suffer from large aberrations and remains diffraction limited. The spot shape is elliptical with a FWHM of 264 nm along the electrical field axis (p plane) and 153 nm perpendicular to it (s plane). The elliptical shape in the focal spot is a consequence of the exact full vector field model calculation as demonstrated by Richard and Wolf.[14,7] Figure 5 shows however that not only most of the reflected energy originates from above the critical angle regions but also that it appears to come from a virtual focal

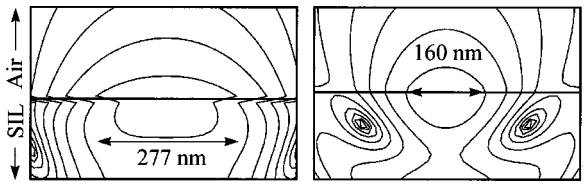

FIG. 5. Field intensity contour lines (a factor 2 between lines) in the vicinity of the focal spot in the p -plane (left) and the s plane (right) calculated at the SIL/air interface for $n=1.76$, $\lambda=633$ nm.

plane about 1.8 μm in air above the SIL face, consistent with the torroidal aberration observed by Lehmann and Maecker.[12] These supercritical field components are blocked by the confocal pinhole, which explains the observed enhanced reflectivity contrast.

A detailed mapping of the field intensity in the vicinity of the focal point shows that in the p plane, the spot size outside the SIL's face depends on the optical index of the object. Its FWHM in this plane varies from 264 nm for air down to 202 nm for $n=1.845$ (i.e., SIL). Such a variation in the spot size could also lead to a polarization dependent enhancement in contrast to confocal imaging. It would be, however, desirable to determine experimentally the exact shape of the spot and its polarization dependence using, for example, fluorescent emission of nm sized dye balls directly dispersed on the SIL surface.

The authors acknowledge lively and useful discussions with R. D. Grober, M. Koch, and S. Ünlü. Financial support was obtained through FOROPTO and the faculty startup funds at the University of Rochester.

[1] S. M. Mansfield and G. S. Kino, Appl. Phys. Lett. **57**, 2615 (1990).
[2] Q. Wu, G. D. Feke, R. D. Grober, and L. P. Ghislain, Appl. Phys. Lett. **75**, 4064 (1999).
[3] B. D. Terris, H. J. Mamin, D. Rugar, W. R. Stundenmund, and G. S. Kino, Appl. Phys. Lett. **65**, 388 (1994).
[4] B. D. Terris, H. J. Mamin, and D. Rugar, Appl. Phys. Lett. **68**, 141 (1996).
[5] L. P. Ghislain and V. B. Elings, Appl. Phys. Lett. **72**, 2779 (1998).
[6] Q. Wu, R. D. Grober, D. Gammon, and D. S. Katzer, Phys. Rev. Lett. **83**, 2652 (1999).
[7] T. R. Corle and G. S. Kino, *Confocal Scanning Optical Microscopy and Related Imaging Systems* (Academic, New York, 1996).
[8] T. D. Milster, J. S. Jo, and K. Hirota, Appl. Opt. **38**, 5046 (1999).
[9] H. K. V. Lotsch, Optik (Stuttgart) **32**, 116 (1970); **32**, 189 (1970); **32**, 299 (1970); **32**, 553 (1971).
[10] T. Tamir and A. A. Oliner, J. Opt. Soc. Am. **59**, 942 (1969).
[11] R. Weigand and J. M. Guerra, Am. J. Phys. **64**, 913 (1996).
[12] G. Lehmann and H. Maeker, Ann. Phys. (Leipzig) **10**, 161 (1952).
[13] H. Maeker, Ann. Phys. (Leipzig) **10**, 115 (1952); **10**, 153 (1952).
[14] B. Richards and E. Wolf, Proc. R. Soc. London, Ser. A **253**, 358 (1959).